Available online at www.academicpaper.org
Academic @ Paper
ISSN 2146-9067
International Journal of Automotive Engineering and Technologies
Vol. 6, Issue 1, pp. 30 – 40, 2017

International Journal of Automotive Engineering and Technologies
http://www.academicpaper.org/index.php/IJAET

Original Research Article

Improving Aerodynamic Performance for a Reliable Wiper System

Sertaç Çadirci[1], Süleyman Emre Ak[2], Buğra Selenbas[3], Hasan Güneş[4]
[1,2,4]Istanbul Technical University, Department of Mechanical Engineering 34437, Istanbul, TURKEY
[3]Teklas Kaucuk A.S., 41400, Kocaeli, TURKEY,

Received 05 September 2016 Accepted 11 March 2017

Abstract

In this study, it is aimed to simulate aerodynamic forces acting on the windshield wiper system on a simplified geometry at different blade angles. Numerical simulations reveal that at critical blade angles, undesired lift forces can reach their peak values. The blade-spoiler geometry is modified in a manner to alter aerodynamic lift and drag coefficients. On a simplified front windshield it is shown that at a blade angle of 40°, lift forces can be converted to pressing forces by implementing suggested modifications. Furthermore λ_2 vortex identification is used to understand the formation of vortex structures at different blade angles. On the other hand, soiling tests are performed both on original and modified wiper geometries and their performances are compared.

Key Words: Aerodynamics, Wiper Blade, Lift Force, Vehicle Safety, Model Development, Soiling Test

Nomenclature

Latin:

A_p	projection area of the wiper [m^2]
C_D	drag coefficient [$= 2F_{Drag}/\rho\, U^2_\infty A_p$]
C_L	lift coefficient [$= 2F_{Lift}/\rho\, U^2_\infty A_p$]
C_i	model constants for $i = 1, 1\varepsilon, 2, 3\varepsilon, \mu$
F_{Drag}	aerodynamic drag force [N]
F_{Lift}	aerodynamic lift force [N]
F_X	aerodynamic force in x-direction [N]
F_Y	aerodynamic force in y-direction [N]
k	turbulence kinetic energy [m^2/s^2]
G_k	generation of turbulence kinetic energy due to mean velocity gradients
G_b	generation of turbulence kinetic energy due to buoyancy
U	uniform free stream velocity [m/s]
u_j	velocity [m/s]

Greek:

α	inclination angle of the windshield [°]
ε	dissipation of turbulent kinetic energy [m^2/s^3]
λ	eigenvalue
μ	dynamic viscosity [kg/ms]
μ_t	turbulent viscosity [$= \rho C_\mu k^2/\varepsilon$]
ρ	density [kg/m^3]
σ	turbulent Prandtl number

*Corresponding author:
E-mail: cadircis@itu.edu.tr

1. Introduction

Because of vast technological developments in automotive engineering, the requirements of this sector in research and development sharply increase. Especially, vehicle components, which must be specified by international regulations are mostly designed according to the requirements of the customers. Since customer specifications change continuously, the suppliers should fulfil these requirements and continuously focus on research and development studies.

The wiper system is one of the vital security components of the vehicle. The wiper system requires high reliability levels and can only tolerate negligible errors. The wiper has a car-specific design and needs to be improved by research and development. The wiping quality and performance are not only checked at static conditions, but also at high-speed dynamic conditions. However, during the wiping process, the driver can be distracted by un wiped regions on the front windshield contaminated by rain water or soil, thus sufficient wiping performance is very important for vehicle safety.

A wiping system consists of basically three components; driving mechanism, wiper arm and wiper blade. The wiper arm transfers the movement to the wiper blade and the wiping process can be achieved by removing water and dirt from the front windscreen by a blade rubber. To do this, the wiper blade should be forced on the windshield with sufficient pressing force. The necessary force is obtained by a spring mechanism within the arm.

With increasing vehicle speed the necessary pressing force, which is provided by the spring mechanism, will decline due to the aerodynamic lift forces acting on the wiper arm and blade. As the lift force increases, the pressing force distribution between the blade rubber and windshield decreases, thus the necessary force cannot be achieved to wipe efficiently. Thus the design of wiper blade is important for the wiping performance at high vehicle speeds to achieve desired wiping quality and sustain vehicle safety. In order to minimize the aerodynamic lift forces, an alternative force in the opposite direction of the lift force must be created and this can be achieved by special spoiler geometries on the blade. Through subtle modifications in the spoiler geometry, pressing forces can be achieved to overcome lift forces. Current wiper blades can work up to vehicle speeds around 160 km/h without apparent problems, however at relatively higher speeds such as 240 km/h, lift forces become much more apparent.

Clarke et al. [1] studied aerodynamic forces acting on windshield wiper system. They carried out water tunnel tests with a 1/20 ratio model, aerodynamic tests in a rectangular duct and wiping tests for flat plate and a realistic car model. They investigated the wiping quality up to a speed of 140 km/h and stated that wiping quality was decreasing with increasing car speed. They recommended the use of an airfoil to reduce lifting forces acting on the wiper blade.

Dawley et al. [2] investigated aerodynamic behavior of different vehicle parts including windshield wiper system. They acquired force data in wind tunnel experiments for conventional type of wiper blades with an airfoil. They investigated how the airfoil's angle of incidence changes aerodynamic lift forces. They concluded that with the increase of the angle of incidence, lift forces acting on the wiper blade can be reduced and after some point even pressing forces can be achieved.

Jallet et al. [3] did both experimental and numerical studies about windshield wiper blades. They used a horizontal flat surface in their study. In their numerical calculations they found out 4 N lift force at 144 km/h for the conventional wiper system and 4.4 N pressing force for the wiper system with a spoiler. Later they validated their numerical results by experiments.

Billot et al. [4] continued the former study in [3] and investigated a new type flat wiper blade on a car geometry which was positioned in the mid-wipe position. For a speed of 160 km/h they calculated 9.8 N lift force for the conventional type wiper blade without a spoiler and 7.4 N lift force for the

wiper blade with the spoiler. For the new flat blade design, they came up with 4.9 N lift force.
Gaylard et al. [5] carried out numerical and experimental studies using a conventional type wiper blade in a sport utility vehicle at different wiping angles with the aim to understand flow and vortex structures near windshield wiper blades.
Yang et al. [6] numerically studied with conventional type wiper blades on a car geometry. They used seven different wiping angles between 0° and 90° with an increment of 15° and worked at three different vehicle speeds such as 30, 50 and 70 km/h. They found out that most lifting forces occur on the driver side between 30° and 45° and the most critical angle for the passenger side was 30°.
Lee et al. [7] investigated the new flat blade design on a half car model numerically. They used four wiping angles and two vehicle velocities such as 170 and 200 km/h. They found out that the highest lift force acting on the wiper blade occurred during 1/2 period of the wiping cycle on driver side and during 1/4 period of the wiping cycle on the passenger side. They also researched the effect of hood tip on drag and lift forces acting on the wiper blade.
The main aim of the study relies on improving the wiping quality of the wiping system for high speed vehicles, thus this numerical study investigates how to decrease aerodynamic lift forces acting on the wiper blades at 240 km/h by applying geometric modifications. The proposed modifications of the wiper parts such as spoiler's curvature, height and the connection type are found to be useful in terms of improved aerodynamic performance. The increased quality of the wiping performance are also tested by flow visualizations and numerical results are validated qualitatively.

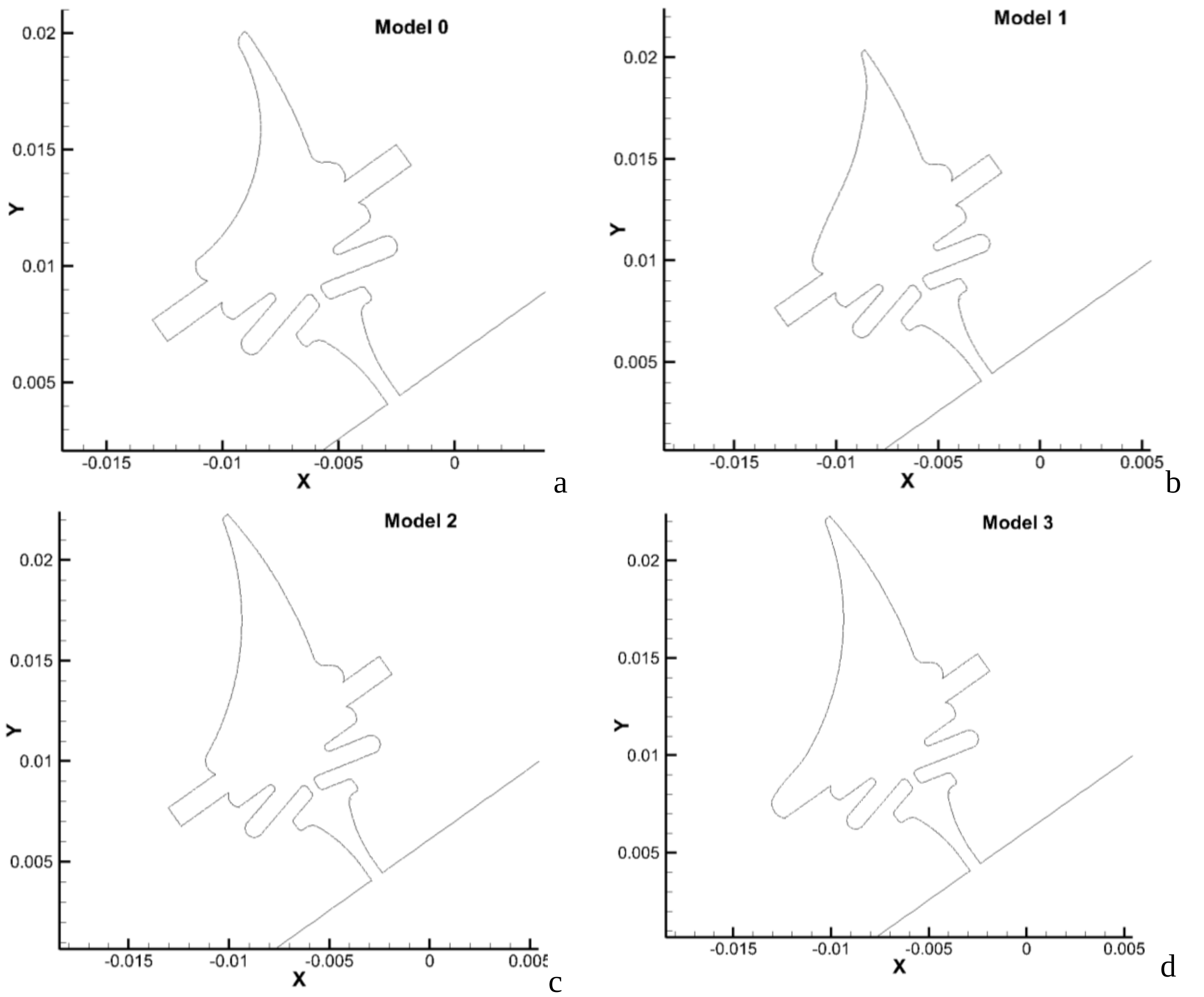

Figure 1: Original and suggested wiper profiles: (a) Model-0, (b) Model-1, (c) Model-2, (d) Model-3

2. Geometry of the Wiper Blades

In the simulations, a simplified model is used and only the wiper blade is taken into account. Four different modifications in the wiper blade design are suggested. Wiper Model-0 is the original wiper with 16.6 mm height. In this model the metal part has sharp edges. Wiper Model-1 has a larger spoiler curvature than Model-0 but has the same height and connection type. Wiper Model-2 has a height of 19 mm and its spoiler curvature and connection type are identical to Model-1. Finally, Model-3 has the same height and spoiler curvature as Model-2. The only difference between Model-2 and Model-3 is the connection type where Model-3 has a rounded metal part (see Figure 1).

Front windshield and hood of the vehicle are represented by two slightly bumped surfaces. The inclination angles between the front windshield and the horizontal plane is approximately 35° (see Figure 2a) and the angle between the windshield and the hood is approximately 158°. The fixed point of the wiper blade is located approximately 415 mm from the leading edge of the hood. The angle of the wiper blade is determined by a horizontal line going through the fixed point of the wiper blade.

3. Computational Studies

3.1. How to calculate forces

For all calculations, aerodynamic drag and lift forces acting on the wipers and their corresponding coefficients are calculated as given in Eq.(1) and Eq.(2) where F_x and F_y are forces in x-and y-directions respectively which are obtained from computations. Here, α represents inclination angle of the windshield where A_p stands for the projection area of the wiper. Figure 2a and 2b show the original wiper and spoiler profile and the computational domain with the imposed boundary conditions respectively.

$$F_{Lift} = F_Y \cos\alpha - F_x \sin\alpha \qquad (1)$$
$$F_{Drag} = F_Y \sin\alpha + F_x \cos\alpha$$

$$C_L = \frac{F_{Lift}}{\frac{1}{2}\rho U_\infty^2 A_p} \; ; C_D = \frac{F_{Drag}}{\frac{1}{2}\rho U_\infty^2 A_p} \qquad (2)$$

a

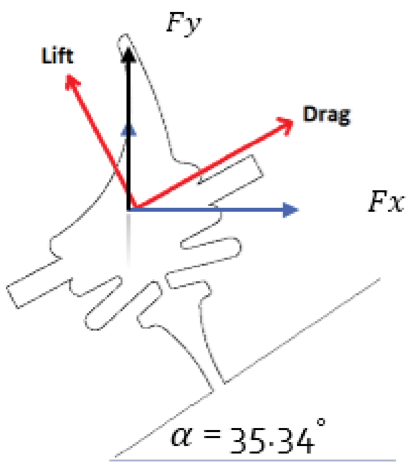

b

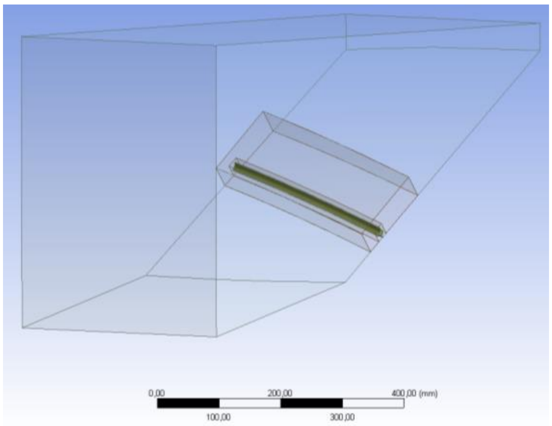

Figure 2: Original wiper geometry: (a) forces acting on windshield wiper, (b) computational domain and imposed boundary conditions.

3.2. Mesh and Convergence Tests

Convenient boundary conditions are defined on the surfaces of the flow domain as shown in Figure 2b. The vertical surface upstream of the wiper blade is prescribed with inlet boundary condition (uniform free stream velocity of 240 km/h) and the upper surface of the domain and the vertical surface opposite to the inlet have outlet boundary conditions. The remaining vertical surfaces on the right and left sides of the wiper blade are defined with symmetry boundary condition. Meshing is done with hexahedral elements where in the vicinity of the wiper blade the mesh is clustered densely which is indicated by a box encapsulating the wiper blade in Figure 2b.

Extensive grid checks have been performed to obtain the mesh which can supply reliable numerical results. Depending on the blade angle, the number of the cells can change however, sufficiently dense meshes consisting of around 13.8 million hexahedral elements are found to be sufficient to obtain reliable results at different blade angles. Table 1 shows the mesh independence tests for the calculated aerodynamic forces and coefficients using various dense meshes. Figure 3 shows the computational domain with hexahedral elements in the vicinity of the wiper blade and mesh for the boundary layer. The convergence criteria for all transport equations is set to be 10^{-5} and Figure 4 shows the convergence of the aerodynamic forces acting on the wiper blade with respect to iterations.

Table 1: Mesh-independence tests for Model-0 (original wiper) at zero wiper angle

Cells [Million]	F_x [N]	F_y [N]	F_{Drag} [N]	F_{Lift}[N]	C_D	C_L
5,3	32,4	30,3	44	5,91	2,23	0,30
7,7	34,1	29,1	44,6	3,96	2,27	0,20
10,2	33	30,6	44,6	5,91	2,26	0,30
13,8	35	28,9	45,3	3,33	2,30	0,17
16	35,6	28,7	45,6	2,83	2,32	0,14

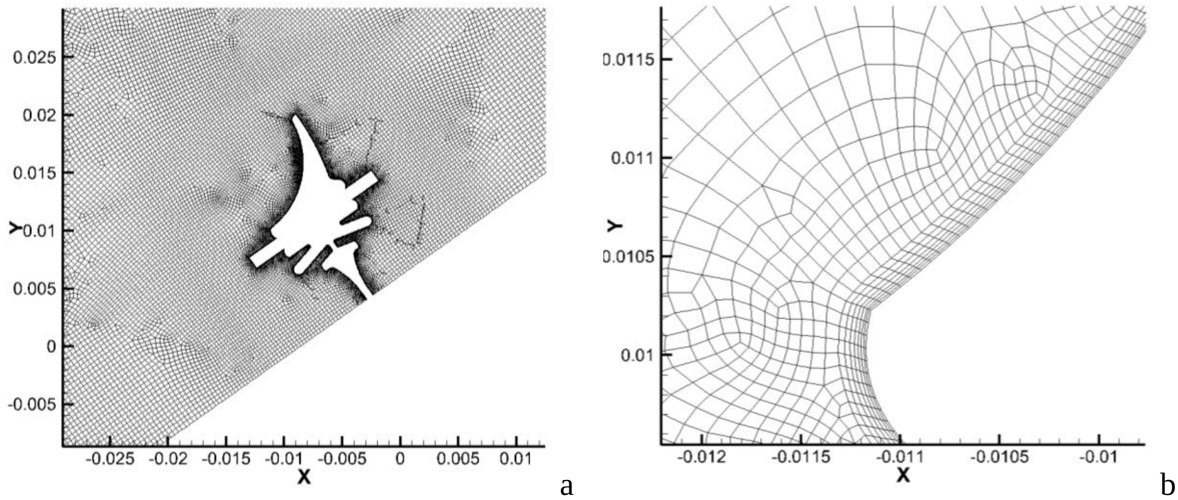

Figure 3: Mesh used in the computations: (a) computational domain near the wiper blade and (b) mesh on the blade surface, both axis are given in (m)

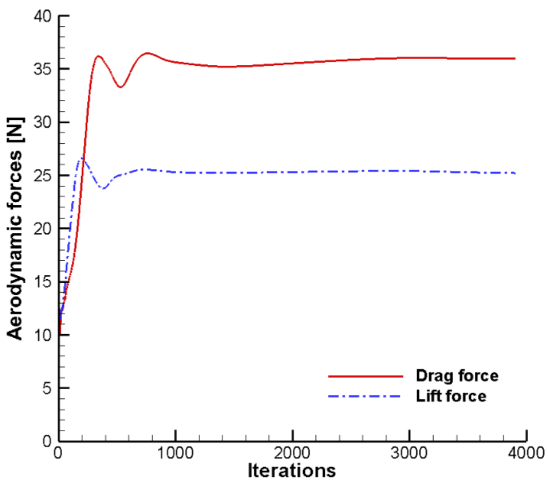

Figure 4: Convergence of aerodynamic forces acting on the wiper blade.

3.3. Computational Approach

The flow is modeled by the finite-volume based, incompressible, turbulent, steady flow solver (ANSYS-Fluent). Realizable k-ε turbulence model is selected with enhanced wall functions where y+ is around 5.

SIMPLE algorithm is preferred with second order upwind schemes for momentum, turbulence kinetic energy and turbulence kinetic energy dissipation equations. The turbulent length scale is assumed to be the height of the spoiler varying between 16.6 mm and 19 mm. Turbulence intensity is assumed to be 3% at the inlet. The fluid is air with constant thermo-physical properties where the density is ρ=1.225 kg/m3 and the dynamic viscosity is μ=1.79x10-5 kg/ms. The Reynolds-Averaged-Navier-Stokes equations are solved together with the transport equations of turbulent kinetic energy (k) and of turbulence kinetic energy dissipation (ε). The transport equations for (k) and (ε) for the Realizable k-ε turbulence model are indicated in Equations (3) and (4) respectively [9].

$$\frac{\partial}{\partial x_j}(\rho k u_j) = \frac{\partial}{\partial x_j}\left[\left(\mu + \frac{\mu_t}{\sigma_k}\right)\frac{\partial k}{\partial x_j}\right] + G_k + G_b - \rho\varepsilon - Y_M + S_k \quad (3)$$

$$\frac{\partial}{\partial x_j}(\rho \varepsilon u_j) = \frac{\partial}{\partial x_j}\left[\left(\mu + \frac{\mu_t}{\sigma_\varepsilon}\right)\frac{\partial \varepsilon}{\partial x_j}\right] + \rho C_1 S\varepsilon - \rho C_2 \frac{\varepsilon^2}{k+\sqrt{\nu\varepsilon}} + C_{1\varepsilon}\frac{\varepsilon}{k} C_{3\varepsilon} G_b + S_\varepsilon \quad (4a)$$

$$C_1 = \max\left[0.43, \frac{\eta}{\eta+5}\right], \eta = S\frac{k}{\varepsilon}, S = \sqrt{2S_{ij}S_{ij}}, S_{ij} = \frac{1}{2}\left(\frac{\partial u_j}{\partial x_i} + \frac{\partial u_i}{\partial x_j}\right); C_{1\varepsilon} = 1.44; C_2 = 1.9; \sigma_k = 1; \sigma_\varepsilon = 1.2 \quad (4b)$$

4. Computational Results

4.1. Effect of Angle on Drag and Lift Coefficients

For all four wiper profiles, it is observed that the variation of the drag coefficient with respect to blade angle indicates the same characteristics as shown in Figure 5a. Highest drag forces are obtained for the Model-3 where lowest drag forces are given for Model-0. However, the trend of lift coefficient variation with respect to blade angle is very similar for Models-0 and Model-1.

Furthermore, Model-2 and Model-3 indicate the same trend in the variation of lift coefficients as given in Figure 5b. In Table 2, aerodynamic forces for the original and modified wiper geometries at horizontal positions are compared. The variation of the lift coefficients for the original Model-0 and the model with an increased spoiler curvature which is Model-1 indicates that lift forces decrease from horizontal position till a blade angle of 20° gradually and then suddenly increase till a blade angle of 40° and reach a peak. Passing 40° the lift coefficients gradually drop till 50°. It should be mentioned that lift coefficients for Model-0 are lowered by approximately 0.1 at all blade angles if Model-1 is preferred instead. Model-2 with a higher blade height and Model-3 with a rounded metal part indicate the same aerodynamic behavior between blade angles 0° and 40° however their lift coefficients do not decline, but keep increasing till 50°.

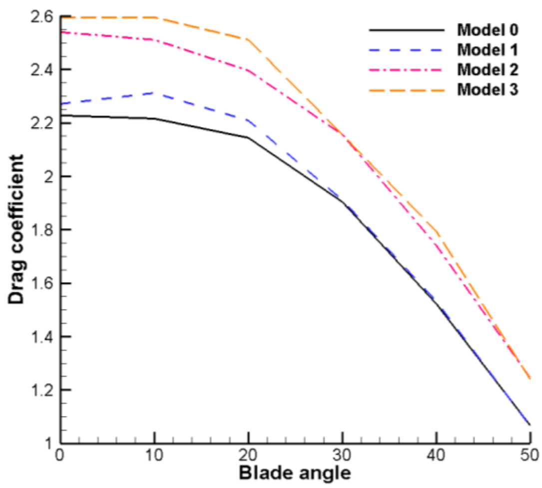

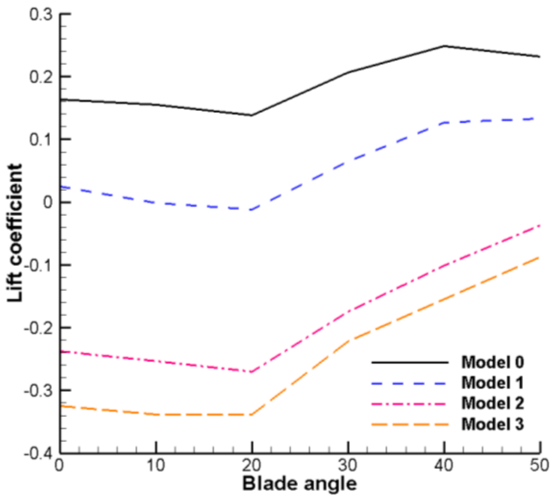

Figure 5: Variation of (a) drag coefficient and (b) lift coefficient with blade angle for different geometries at 240 km/h

Table 2. Comparison of aerodynamic forces for the original and modified wiper geometries at a blade angle of 0° (horizontal position).

Wiper	F_x [N]	F_y [N]	F_{Drag} [N]	F_{Lift} [N]	C_D	C_L
Model-0	35.0	28.9	45.3	3.34	2.23	0.16
Model-1	37.4	27.1	46.2	0.52	2.27	0.03
Model-2	51.4	29.6	59.0	-5.54	2.54	-0.24
Model-3	53.6	28.8	60.4	-7.56	2.60	-0.33

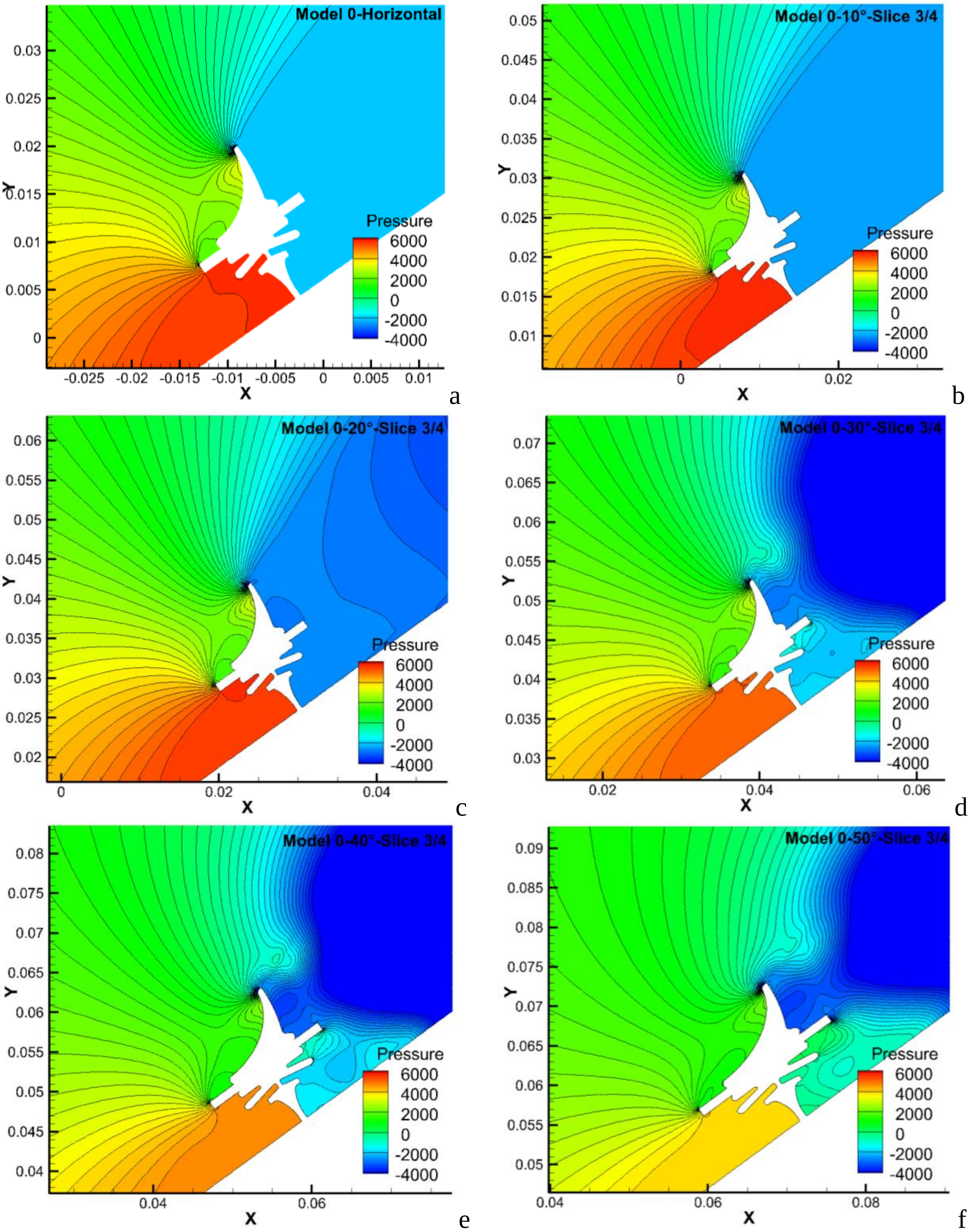

Figure 6: 3/4 sectional view of pressure contours in [Pa] for Model-0 at different blade angles (a) horizontal, (b) 10°, (c) 20°, (d) 30°, (e) 40° and (f) 50°

Pressure contours in Figure 6 displays numerical results obtained for the original geometry (Model-0) at different blade angles. With increasing wiper angle, pressure values upstream of the wiper and over the spoiler are decreasing. Also a visible negative pressure zone can be seen downstream of the wiper blade after an angle of 30°. This can be explained by vortex structures forming past the wiper blade.

In Figure 7 pressure contours at 30° blade angle for the modified wiper models can be seen. Model-2 and Model-3 have higher pressure values above their spoilers and this is an indication for a better performance where undesired lift forces are reduced.

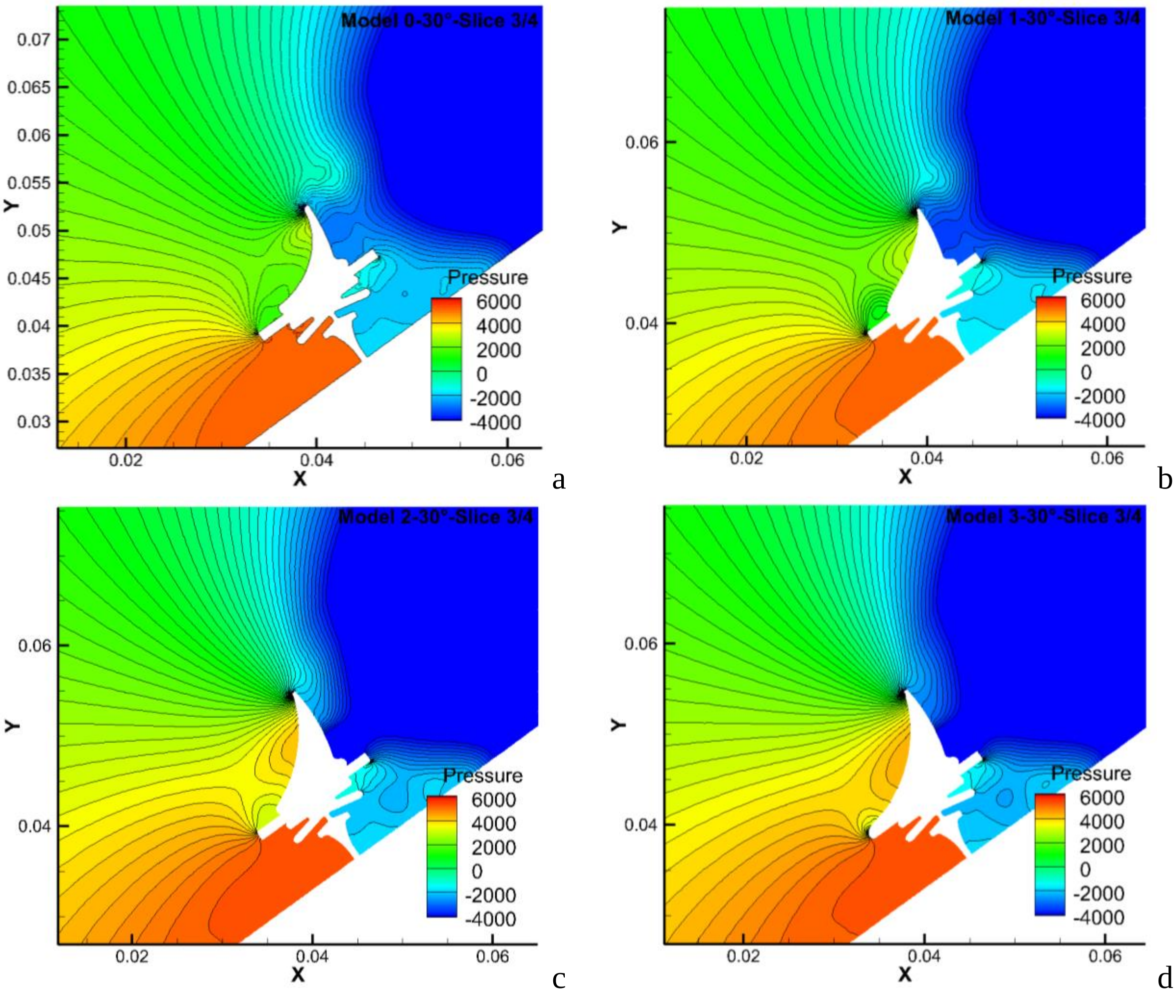

Figure 7: 3/4 sectional view of pressure contours in [Pa] for 30° blade angle (a) Model 0, (b) Model 1, (c) Model 2, (d) Model 3

4.2. λ_2 Vortex Identification Method

There are several vortex identification methods, one of them which is λ_2 vortex identification. It is utilized to reveal detailed flow structures. Pressure differences caused by them can be seen in Figure 8 where contours are shown in the 3/4 slices of the geometry. λ_2 vortex criterion is a detection algorithm that can adequately identify vortices from a three-dimensional velocity field. It consists of several steps: first the velocity gradient tensor is defined and then the tensor is decomposed into its symmetric and anti-symmetric parts, both parts are obtained by the velocity tensor and its transpose. Next for each point in the velocity field three eigenvalues are calculated and ordered in descending order. A point in the velocity field is part of a vortex core only if at least two of its eigenvalues are negative, or $\lambda_2 < 0$ [8].

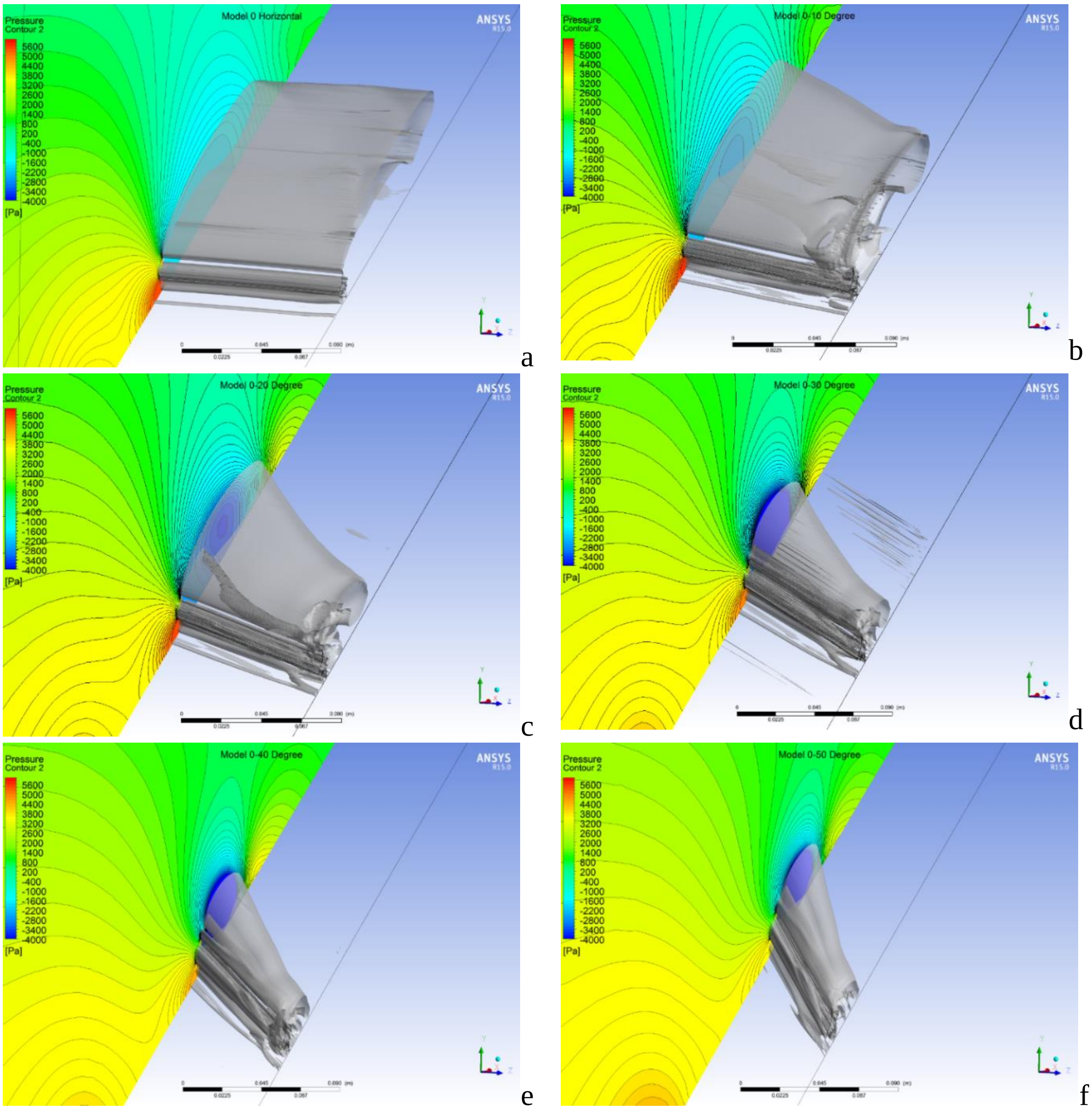

Figure 8: Pressure contours in [Pa] from 1/4 slice of the geometry and iso-surfaces for vortex determenitaion critierion λ_2=0.001 (a) 0º, (b) 10º, (c) 20º, (d) 30º, (e) 40º and (f) 50º; to identify vortex structures λ_2 criterion [8] is used

5. Experimental Results

Soiling tests have been carried out in a thermal wind tunnel to compare the performances of the original wiper blade with the performance of the modified wiper blades. To obtain more reliable experimental results, the spring preload is initially measured by a force-meter (10.7N) before applying aerodynamic forces in the wind tunnel. Flow visualizations are done by UV-light where water droplets with fluorescent agent are added to the air flow. Evaluation and qualification of the resulting soiling tests are done. Figure 9 shows instantaneous snapshots captured during soiling tests where the wiper blades are located at the possible lowest and highest positions in the wiping cycle. Modified wiper (Model-3) with a better aerodynamic performance is found to be more satisfactory than the original wiper model since the water spots on the windshield disappear at high speeds.

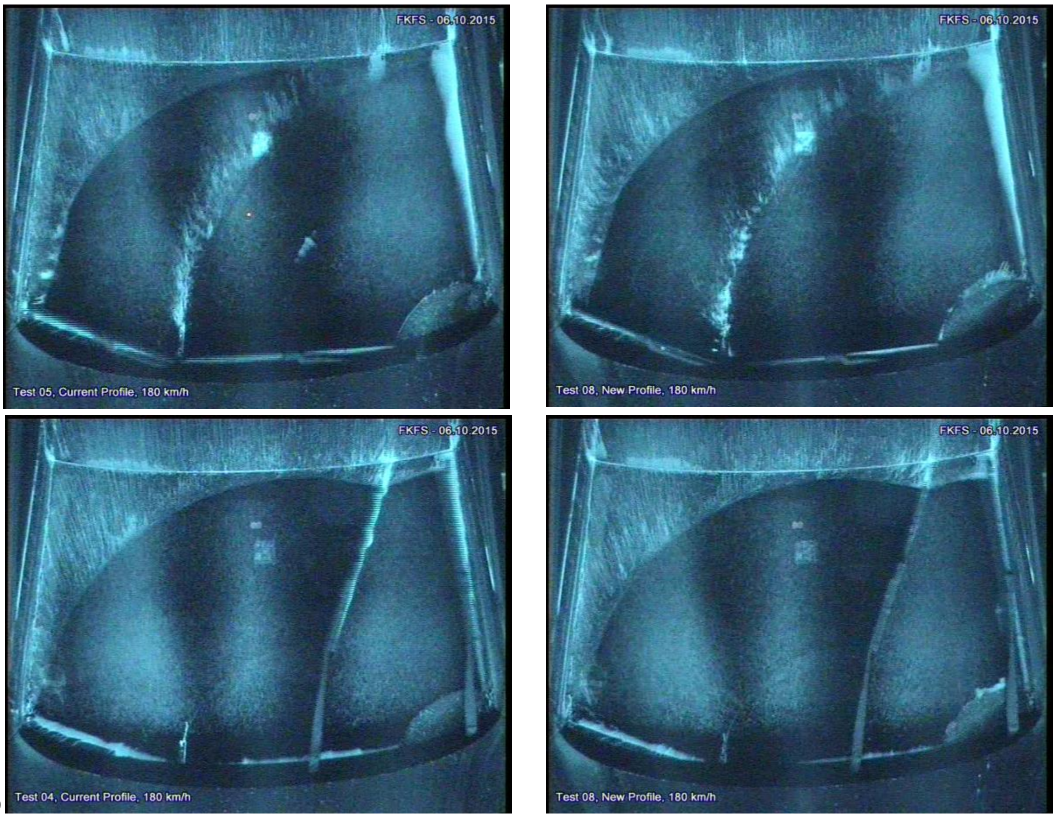

a

b

U = 180 km/h (lowest and highest positions)

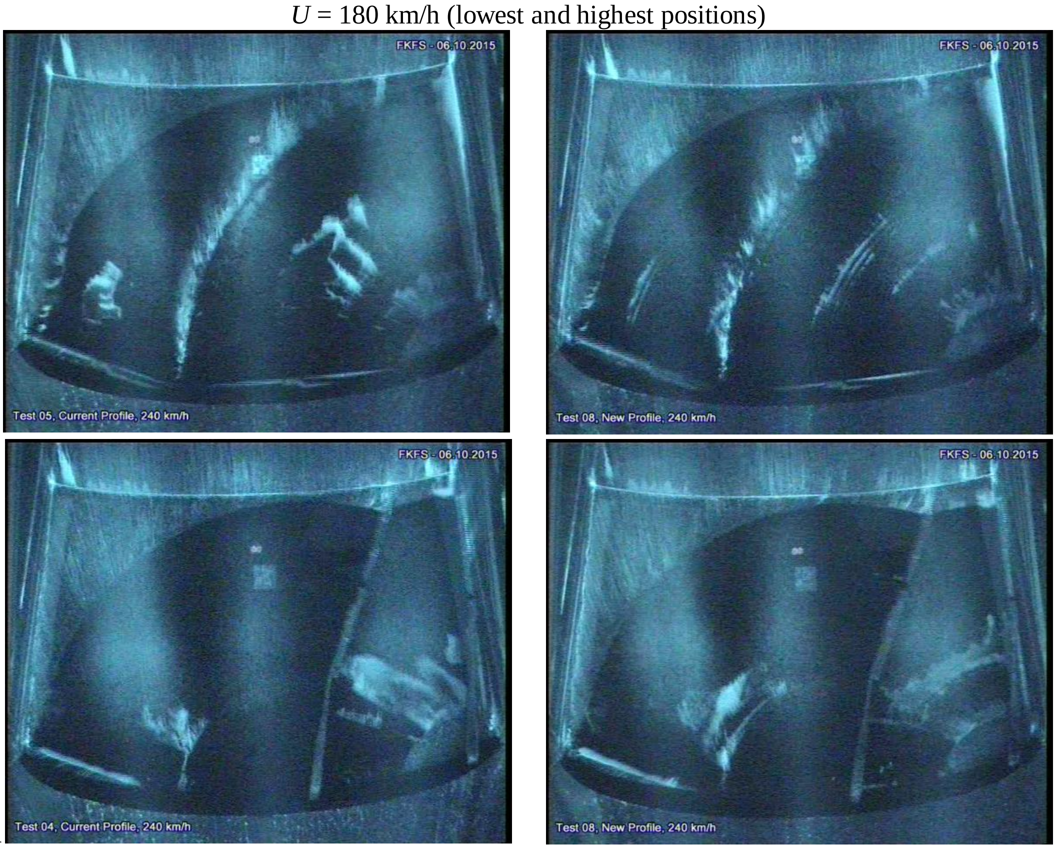

c

d

U = 240 km/h (lowest and highest positions)

Figure 9: Captures from wiping test, left coloumn for the original wiper and right coloumn for the modified wiper: (a) 180 km/h, wiper blades at lowest position, (b) 180 km/h, wiper blades at highest position, (c) 240 km/h, wiper blades at lowest position, (d) 240 km/h, wiper blades at highest position.

6. Conclusion and Discussion

In this paper aerodynamic forces acting on the wiper blades with different modified geometries are investigated numerically and experimentally. The main goal of the study is to generate down forces to overcome lifting at high speeds. Three geometric parameters are investigated: spoiler curvature, wiper height and connection type. It is revealed numerically that an increased wiper height with a rounded metal part supply most satisfactory results in terms of decreased lift forces at various blade angles. Pressing forces on the wiper system are achieved if the suggested models are used. Soiling test are carried out in a thermal wind channel where the proposed wiper blade modification supplies much more satisfactory results in terms of better vehicle safety. As extensive numerical investigations and soiling tests revealed, Model-3 is found to be the best modification and it is manufactured.

Acknowledgments

The authors are indebted to Ministry of Science, Industry and Technology of Turkey and Teklas Kaucuk A.S. for financial support through the project 0278-STZ-2013-2 and Forschungsinstitut für Kraftfahrwesen und Fahrzeugmotoren (FKFS) University Stuttgart, Germany for giving us the permission to use their thermal wind tunnel.

7. References

[1] Clarke, J. S. and Lumley, R. R. "Problems Associated With Windscreen Wiping". Paper 600134, SAE Summer Meeting, Edgewater Beach Hotel, Chicago, Ill., June 5-10, 1960.

[2] Dawley, M. W., "Aerodynamic Effects on Automotive Components". Paper 650134, International Automotive Engineering Congress, Detroit, Michigan, January 11-15, 1965. Society of Automotive Engineers Inc.

[3] Jallet, S., Devos, S., Maubray, D., Sortais, J-L, Marmonier, F., and Dreher, T., "Numerical simulation of wiper system aerodynamic behaviour". SAE Paper 2001-01-0036. SAE 2001 World Congress, Detroit, Michigan, USA, 03/05/2001 - 03/08/2001. Society of Automotive Engineers, Inc., Warrendale, Pennsylvania, USA.

[4] Billot, P., Jallet, S., and Marmonier, F. "Simulation of aerodynamic uplift consequences on pressure repartition~Application on an innovative wiper blade design." SAE Paper 2001-01-0043. SAE 2001 World Congress, Detroit, Michigan, USA, 03/05/2001 - 03/08/2001. Society of Automotive Engineers, Inc., Warrendale, Pennsylvania, USA.

[5] Gaylard A. P., Wilson A. C., & Bambrook G. S. J. (2006) A Quasi-Unsteady Description of Windscreen Wiper Induced Flow Structures. Paper presented at 6th MIRA International Vehicle Aerodynamics Conference, October 2006, Nuneaton: MIRA Ltd.

[6] Z. G. Yang, X. M. Ju, and Q. L. Li, "Numerical Analysis on Aerodynamic Forces on Wiper System". Proceedings of the Sixth International Conference on Fluid Mechanics, AIP Conf. Proc. Vol 1376, 213-217 (2011).

[7] Seung Ho Lee, Sung Won Lee, Sang Hyuk Lee, Nahmkeon Hur, Woo-Nyoung Choi and Jin-Hwan Sul, "(In Korean) A Numerical Study on the Aerodynamic Lift of the Windshield Wiper of High-speed Passenger Vehicles," The Proceedings of Asian Symposium on Computational Heat Transfer and Fluid Flow 2009, Vol.3, pp.185-190, Jeju (Oct. 2009).

[8] Jeong, J. and Hussain, F. "On the identification of a vortex". Journal of Fluid Mechanics, (1995), 285, pp. 69-94.

[9] ANSYS Fluent Theory Guide Release 15, pp.2,3,51-54, 2013.